Proceedings of the ASME 2012 31st International Conference on Ocean, Offshore and Arctic Engineering
OMAE2012
July 1-6, 2012, Rio de Janeiro, Brazil

OMAE2012-84270

FATIGUE OF FRICTION STIR AND GTAW WELDED AZ31B MAGNESIUM ALLOY

J. A. Ávila*
Ingeniería de Materiales
Universidad del Valle,
Cali, Colombia

H. E. Jaramillo
Departamento de Energética y Mecánica, Universidad
Autónoma de Occidente
Cali, Colombia

F. Franco
Ingenieria de Materiales
Universidad del Valle,
Cali-Colombia

ABSTRACT

The mechanical behavior of butt welds made on AZ31B magnesium alloy plates by solid-state friction stir welding (FSW) and gas tungsten arc welding (GTAW) is presented. Fatigue, tensile strength, and hardness tests were performed. Also, fractographic analyses of the weld microstructures were conducted. Tests results show that the fatigue performance of FSW joints was superior to that of conventional welding (GTAW).

Keywords: FSW; GTAW; AZ31B; magnesium alloys; fatigue behavior; fractography

NOMENCLATURE

BM: Base Material
EDS: Energy Dispersed Spectroscopy
FZ: Fusion Zone
FSW: Friction Stir welding
GTAW: Gas Tungsten Arc Welding
HAZ: Heat Affected zone
HV: Vickers hardness
SEM: Scaning Electron Macroscopy
SZ: Stirred Zone
TMAZ: Thermomechanically Affected Zone

1 INTRODUCTION

Magnesium alloys possess high specific mechanical strength, good machinability and can be recycled [1]. These alloys have a great potential to be implemented in the design of metallic structures where aluminum alloys are currently used [2, 3]. Even in the automotive industry, magnesium alloys have become attractive due to their low weight, making vehicles more fuel efficient [4].

These Mg alloys can be welded using a conventional fusion process, but tend to present, at the microscopic level, cracks, pores, and voids [5]. Therefore, FSW can be used instead to improve on those shortcomings. The FSW process consumes a very small amount of energy and does not make use of neither shielding gases nor consumables materials. The FSW process also exhibits superior mechanical properties when compared to conventional welding [6].

The main purpose of this investigation was to compare the fatigue behavior between Mg AZ31B alloy welded by a conventional GTAW process and a particular FSW set up using a milling machine. Various authors [7, 8; 9] investigated the mechanical behavior of different welded metals, including AZ31B Mg alloy, using FSW and fusion welding process. They all found better mechanical performance in those metals welded with FSW compared to GTAW joints.

2 EXPERIMENTAL PROCEDURE

2.1 Material:

Extruded plates of AZ31B Mg alloy 90-mm wide x 120-mm long x 3.20-mm thick were selected to make the butt-welded samples. The butt joints for both welding procedures did not have any bevel angle other than straight edges (90º). The chemistry of the base Mg metal is given in Table 1.

2.2 Welding:

The friction stir welding was carried out using a welding speed (V_A) of 159 mm/min, rotating speed (V_R) of 1600 RPM, and a pitch angle of 1°. A Nangtong X6125A milling machine was employed and adjusted for application of friction stir welding. The welding direction for both FSW and GTAW was perpendicular to the direction of the extruded plates. For the

*Author of correspondence

Copyright © 2012 by ASME

Downloaded From: http://proceedings.asmedigitalcollection.asme.org/pdfaccess.ashx?url=/data/conferences/asmep/75837/ on 06/13/2017 Terms of Use: http://www.asme.org/abo

FSW, the abutting plates were held together without any gap in the horizontal position perpendicular to the axis of the rotating tool. The plates were advanced in a way that the rotating tool traversed the plate width.

The GTAW was performed using a ESAB Heliarc 252 welding machine. The welding parameters used were:15V, 59 A, 3.83 mm/s, and the flow of Argon fixed at 20 CF; during the procedure alternate current and high frequency were also used. The filler wire used was ER AZ61A in braided form using three wires of 1.6 mm in diameter. The yield strength and mechanical strength of wire was 228 and 310 MPa, respectively [10]. The chemical compositions of the base metal (BM) and filler metal are given in Table 1.

Table 1. Chemistry of plate and wire [%]

Alloy	*Al*	*Mg*	*Fe*	*Mn*	*Si*	*Zn*
AZ31B	2.8	Bal	0.007	0.52	0.09	1.0
ER AZ61A	6.5	Bal	---	0.2	---	1.0

Welding was applied in such a way that is perpendicular to the cross-section of the joints. For the specimens welded using GTAW two passes were used. The microstructure photos were taken using an Olympus PMEU optical microscope, and samples were etched for contrast purposes using 4.2 g of picric acid, 10 ml acetic acid, 10 ml H_2O, and 70 ml ethanol (95%) [7].

2.3 Hardness Tests:

Hardness measurements in the welded area were carried across the weld section at mid thickness of the weld cross-section. For these measurements a Wilson 401 MVD microhardness tester was employed, using 1 mm separation between indentations, with 100 gr of load during 10 s.

2.4 Tensile Tests:

The tensile tests were carried out using a continuous radius between the ends of the specimens, according to ASTM E466 standards. The specimens for both the tensile and fatigue tests were taken across the weld in the longitudinal direction of the welded plate. The tensile tests were performed using a universal Instron testing machine (3366 series) at a constant strain rate of 1 mm/min, according to the standard ASTM E8M [11].

2.5 Fatigue Tests:

Fatigue tests were conducted for the base material, FSW and GTAW joints. Stress Ratio equal to 0.1 (R=0.1) and frequency of 10 Hz at room temperature in air were employed [12]. Upon failure, the fracture surfaces were examined under a Scanning Electron Microscope (SEM) JEOL JSM 6490LV attached with energy dispersed spectroscopy (EDS) system.

3. RESULTS AND DISCUSSION

3.1 Macrostructural and Microstructural Features:

The macrostructural study of GTAW and FSW joints was performed in a previous study [10, 13]. The aforementioned study found that the FSW process was free of macrostructural defects (parameters in their study were V_A=159 mm/min and V_R=1600 rpm). However, pores were observed in the fusion zone of the GTAW joints due to the nature of the welding process [14].

These grains have a mean diameter of 50 µm, as seen in Figure 1.a. Several non-metallic inclusions scattered and orientated were also found in the base metal (BM) during the extrusion process. According to the EDS analysis the non-metallic particles were composed of Al_xMn_y similar findings were reported in the past [15].

GTAW Features: The GTAW joint showed two different microstructure zones: The heat affected zone (HAZ) and the fusion zone (FZ) [16]. The FZ microstructure presented equiaxial fine grains with a second phase precipitates in grain boundaries (Figure 1.b). Precipitates of Al_xMg_y were also verified through EDS analysis. The HAZ showed decrease in grain size and change in shape under the presence of second phase precipitates.

Table 2. Average grains sizes in BM, FZ and SZ.

Zone	*Av. Grain size ASTM*	*Av. diameter (µm)*
MB	5	50
FZ	8	18
SZ	11	7

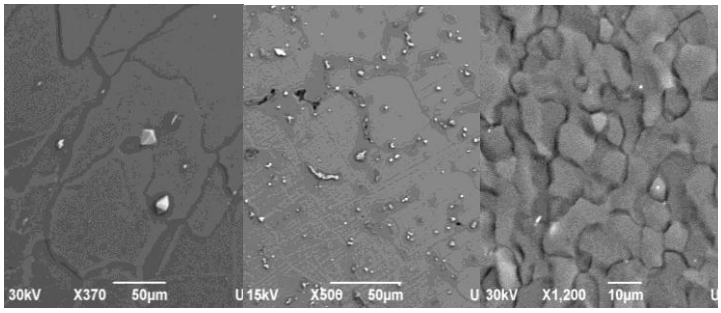

a.) b.) c.)

Figure 1. Typical Microstructures: a.) Base metal; b.) Fusion zone; and c.) Stirring zone.

FSW Features: The FSW joints were divided in three different microstructure zones, stirred zone (SZ), thermomechanically affected zone (TMAZ), and heat affected zone (HAZ). The SZ presented equiaxial fine grains with mean grain diameter of 7 µm due to dynamical recristallization [6], this zone is shown in Figure

Copyright © 2012 by ASME

Downloaded From: http://proceedings.asmedigitalcollection.asme.org/pdfaccess.ashx?url=/data/conferences/asmep/75837/ on 06/13/2017 Terms of Use: http://www.asme.org/abo

1.c. The TMAZ displayed mixture of equiaxial grains elongated and oriented in direction to the walls of the welded zone, it presented partial dynamic recrystallization due to the thermal deformation of this zone. The HAZ zone was small and difficult to detect, due to the grain change during the FSW process, the Mg AZ31B alloy was very small or non-existent in this zone. Table 2 showed that the grain size average decreased in 86% for SZ and 64% for FZ using a BM mean grain diameter as reference.

3.2 Hardness:

The hardness values in BM showed wide scattering and did not show steady behavior, having a mean Vickers hardness of approximately 50 HV. Betancourt et al. [7] reported similar results. The hardness presented minor variability in SZ and FZ. Figure 2 exhibit Vickers hardness of 47.7±0.8 and 54 ±4 Hv respectively for SZ and FZ.

The GTAW specimens showed higher hardness due to the fact that the metal filler had more Al component precipitates present in the grain boundaries. The AlxMgy precipitates display a great dispersion, increasing the strength which results in a reduction of toughness.

3.3 Tensile properties:

Tests were carried out in the joints until failure occurred for TMAZ and HAZ using FSW and GTAW processes, respectively. Table 3 gives the tensile properties for base and weld metals as tested. The efficiency (η) is defined as the weld-to-parent metal tensile strength ratio. The FSW joint showed an efficiency of 90%, with elongations of approximately 3.2%, while the GTAW specimens yielded higher elongation and ultimate tensile strength . This may be attributed to the presence of Al_xMg_y precipitates in the GTAW weld.

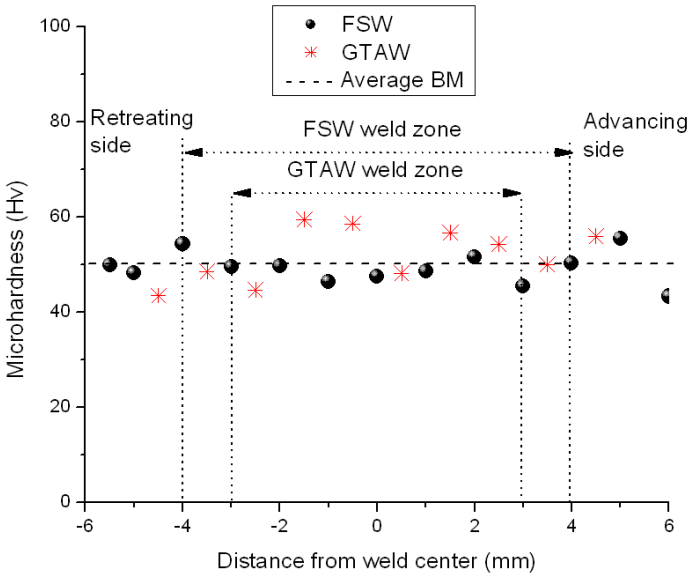

Figure 2. Typical hardness profiles of FSW and GTAW welds

3.4 Fatigue behavior:

The stress ranges used for the fatigue tests are also provided in Table 3. Table 4 summarizes the test results and Figure 3 presents the fatigue data on a S-N plot. The curves in Figure 3 are least-square fits to each set of data of the Basquin´s equation log (N) = log *(A)+m log* (S_R), where ***N*** is the number of cycles to failure in fatigue tests, ***A*** the intercept, and ***m*** the slope of the curve [17, 18].

As expected, the base metal outperformed both welds consistently over all stress ranges tested. The slope for FSW welds was about the same as (just slightly shallower) that of BM, but consistently below it, while more distinctly shallower than the one obtained for GTAW. This indicates that, for the application at hand, the FSW offers better fatigue performance than GTAW. As expected, the GTAW and FSW joints show somewhat more variance than the BM by 10% and 6%, respectively.

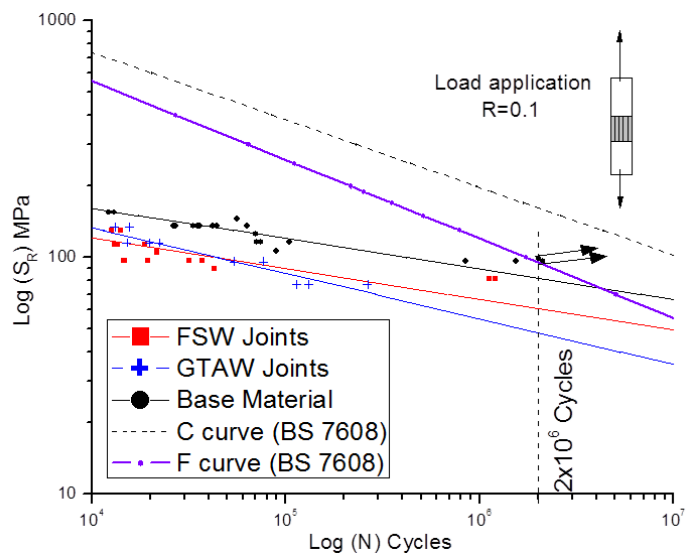

Figure 3. N curves for FSW, GTAW, Base material, and C and F curves of BS 7608 steel code.

On a more quantitative basis, the fatigue strength for the base material was 81 MPa at $2x10^6$ cycles, as compared to the FSW and GTAW joints that exhibit a decrease of 26% and 40% relative to the BM fatigue behavior. These results are similar to those found by Padmanaban et al. [9], who reported a decrease in fatigue behavior of 32% for FSW joints and 45% for the GTAW joint compared to BM. For the sake of comparison, the C and F S-N mean curves of BS 7608 steel code for high and low weld qualities applicable to butt fusion welds in steel are also shown in Fig. 3. Recognizing the difference in material properties between Mg alloys and steel, it may be said that there may be an incentive to use FSW to steel applications to improve fatigue life.

Copyright © 2012 by ASME

Downloaded From: http://proceedings.asmedigitalcollection.asme.org/pdfaccess.ashx?url=/data/conferences/asmep/75837/ on 06/13/2017 Terms of Use: http://www.asme.org/abo

Table 3. Summary of the mechanical properties of BM, FSW and GTAW joints.

Specimen	*V_R (rev/min)*	*V_A (mm/min)*	*Su (MPa)*	*Elongation (%)*	*η (%)*	*Ranges evaluated in fatigue test (MPa)*
BM	---	---	215	12.9	100	155, 135, 116, 97
FSW	1600	159	194	3.2	90	130, 113, 97, 81
GTAW	---	230	212	5.9	99	153, 134, 115, 96, 77

Table 4. Summary of fatigue properties of BM, FSW and GTAW joints.

Specimen	*m*	*Fatigue Strength 2x106 cycles (MPa)*	*Tests to failure*	*Run out Tests (No failure)*	*Standard deviation of log N*
BM	-7.83	81	19	2	0.516
FSW	-7.79	60	14	0	0.567
GTAW	-5.203	48	16	0	0.605

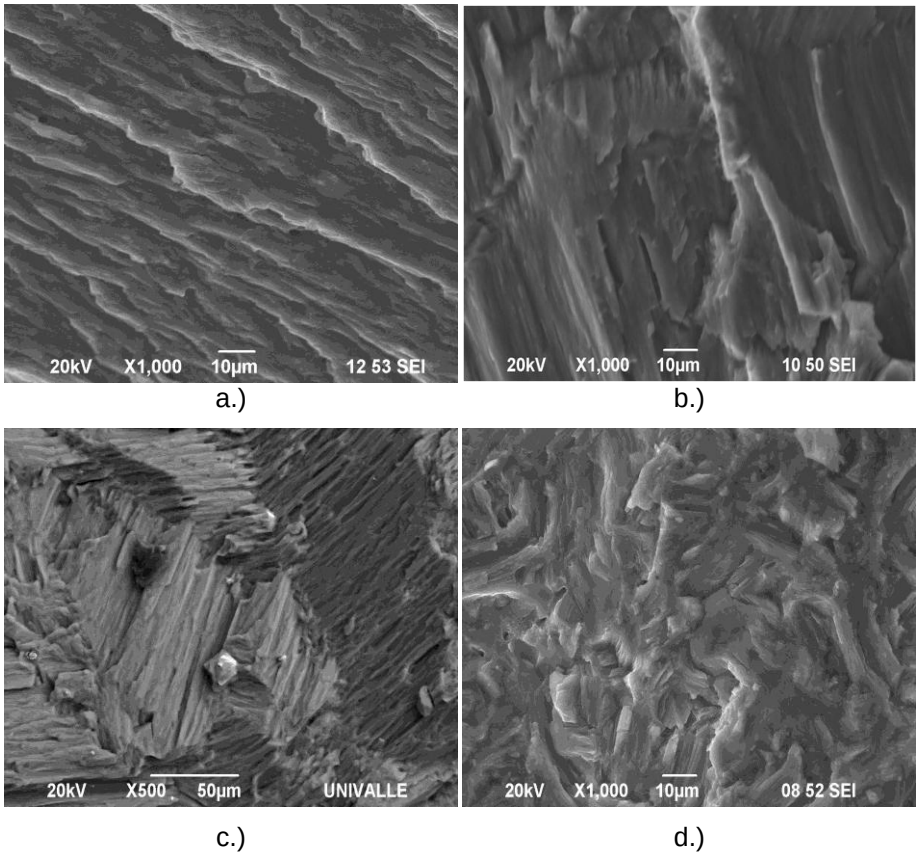

Figure 4. Typical SEM images of fatigue fracture section of FSW, through of fracture section 1 (a.) and fracture section 2 (b.). Compared with Base metal (c.) and GTAW (d.)

3.5 Fractography:

The presence of non-metallic particles (AlxMny) or surface roughness serves as the nucleation of crack that then may propagate into different regions during fatigue testing until fracturing of the BM takes place. Figure 5.a) shows cracks propagating on distinct multiple fractures paths. The fracture paths were oriented in crystallographic planes [19], characteristic of fatigue fractures.

Figure 5 shows the typical fatigue fractured sections of the FWS samples. Two distinct crack initiation sites are identified. The fracture site 1 is located in the root side of the weld between TMAZ and SZ on the sample face opposite to the welding side.

Copyright © 2012 by ASME

Downloaded From: http://proceedings.asmedigitalcollection.asme.org/pdfaccess.ashx?url=/data/conferences/asmep/75837/ on 06/13/2017 Terms of Use: http://www.asme.org/abo

The crack in this zone initiated and propagated due to micro root defects in SZ.

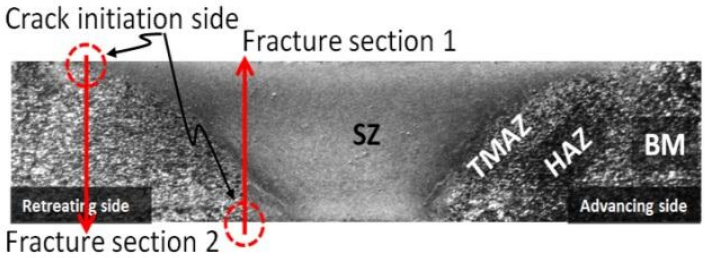

Figure 5. Macro-section view of FSW identifying fatigue fracture sections [13].

Fracture section 2 is between TMAZ just subsurface to the welding side and can be attributed to grain size and orientation and the presence of non-metallic particles in this region. Figures 4 (a) and (b) show the fractured surface patterns for sections 1 and 2, respectively. It should be noted that, along section 1in the FSW, the crack propagated in trans-crystalline planes having a parallel striation pattern in the direction of propagation. The spacing between striations was of approximately 10µm which is in agreement with the SZ.

No macro root defects were observed in the SFW. 64% of the failures initiated in the advancing side, which means that the principal reason for failure was the mechanical and microstructural properties in the TMAZ followed by micro-roots defects. Failure in the GTAW specimens occurred inside the fusion zone. The reason for the principal crack initiation was micro-cracks between precipitate phases; crack growth was similar to BM (see Figure 4.c) but more arbitrary and smaller compared to BM, probably due to the fast and disorganized solidification process in fusion welding.

4 CONCLUSIONS

A testing program aimed at comparing the tensile strength and fatigue performance of AZ31B Mg alloy welded via FSW and GTAW processes was completed.

The mechanical strength of FSW specimens was 90% of the BM, while in GTAW achieved 99% of BM. In fatigue, however, FSW outperformed the GTAW, as indicated by a shallower slope of the SN curve obtained for FSW , -7.8, compared to -5.2 for GTAW. Compared to the base material, the fatigue life evaluated at 2×10^6 cycles for FSW decreased by 26% while GTAW joints decreased by 40%.

Equiaxial fine grains were revealed. Fully grains dynamically recrystallized for FSW welds allow biggest grain size decrease for SZ than FZ. The GTAW in the FZ microstructure presented second phase precipitate in grain boundaries because the weld zone had more Al alloy. Microhardness of FZ was higher than SZ due to the presence of a precipitate phase in grain boundary

SEM analyses of fractured surfaces suggested that the principal cause of failure for BM was the presence of non metallic particles. In the case of FSW joints, fatigue failure occurred in two different regions and it was attributed to micro-roots defects, non-metallic particles and the disparity in mechanical properties of TMAZ. The pores and micro-cracks between precipitate phases facilitated the premature failure by fatigue during the testing of joints using the GTAW process. The GTAW fatigue fractures are show in the Figure 4 (d)

5 ACKNOWLEDGMENTS

The authors acknowledge the kind support of the Mechanical Engineering Department of the Universidad Autónoma de Occidente, and the Materials Engineering School of the Universidad del Valle. Also duly acknowledged are the contributions of Resconstructura Alemana with the GTAW welding process and of Jaime Buitrago, of ExxonMobil Upstream Research, with the analysis of the fatigue test results and editorial reviews.

6 REFERENCES

[1] Franco, F., Sánchez, H., Betancourt D., and Murillo, O., 2009, *Rev. LatinAm. Metal Mater*, **S1 3**, pp. 1369-1375.

[2] Kainer K., 2003, *Magnesium Alloys and Technology*, Wiley-VCH Verlag GmbH & Co KG aA, Germany.

[3] Amú, M., and Franco, F., 2009, *Rev. LatinAm. Metal Mater*, **S 12**, pp. 767-772.

[4] Chowdhury, M., Chen, D., Bhole, S., Cao, X., Powidajko, E., Weckman, D., and Zhouc, Y., 2010, *Mater Sci Eng*, **527**, pp. 2951–2961.

[5] Afrin N., Chen, D., Cao, X., and Jahazi M., 2008, *Mater Sci Eng*, **472**, pp. 179–186.

[6] Mishraa, R. and Mab, Z., 2005, *Mater Sci Eng*, **R 50**, pp. 1-78.

[7] Betancourt, D. and Sanchez, H., 2008, *Evaluación metalúrgica y mecánica de soldadura por fricción agitación en la aleación AZ31B*, Undergraduate Thesis, Universidad del Valle. Facultad de Ingeniería, Escuela de Ingeniería de Materiales, Cali, Colombia, pp. 50-60.

[8] Zhao, J., Jiang, F., Jian, H., Wen, K., Jiang, L. and Chen X., 2010, *Mater & Desing*, vol. 31, pp. 306–311.

[9] Padmanaban, G. and Balasubramanian V., 2010, *Mater & Design*, Vol. **31**, pp. 3724–3732.

[10] Ávila, J.A., Jaramillo, H.E. and Franco, F., 2010, *El Hombre y la Máquina*, Vol. **35**, pp.166-171.

[11] ASTM E 8/E 8M – 08, 2008, *Standard Test Methods for Tension Testing of Metallic Materials. American Society for Testing and Materials*

[12] ASTM E739-91, 2004, *Standard practice for statistical analysis of linear or linearized stress-life (S–N) and strain-life (e-N) fatigue data. American Society for Testing and Materials.*

[13] Ávila, J.A., Franco, F.; and Jaramillo, H.E., 2012, *Rev. LatinAm. Metal*, Vol. **32**, no. 1, pp. 71–78.

Copyright © 2012 by ASME

Downloaded From: http://proceedings.asmedigitalcollection.asme.org/pdfaccess.ashx?url=/data/conferences/asmep/75837/ on 06/13/2017 Terms of Use: http://www.asme.org/abo

[14] Moreira, P.M.G.P., Figueiredo, M.A.V. and Castro, P.M.S.T., 2007, *J. Theor Appl Fract Mech*, Vol. **48**, pp. 169–177.
[15] Friedrich, H., and Mordike, B., 2006, *Magnesium Technology: Metallurgy, Design Data, Applications*, Springer-Verlag Berlin Heidelberg, Germany.
[16] Gang, S., Liming, L., and Peichong, W., 2006, *Mater Sci Eng*, Vol. **429**, pp. 312–319.
[17] Lee, Y.L., Pan, J., Hathaway, R.B., and Barkey, M.E., 2005, *Fatigue Testing and Analysis*. Elsevier Butterworth–Heinemann, USA, pp. 103-180.
[18] Morgado, T., Branco, C., and Infante, V., 2007, *Mecânica Experimental*, Vol. **14**, pp. 35-43.
[19] Engel, L., and Klingele, H., 1981. *An atlas of metal damage: Surface examination by scanning electron microscope*, Wolf Science Books, UK.

Copyright © 2012 by ASME

Downloaded From: http://proceedings.asmedigitalcollection.asme.org/pdfaccess.ashx?url=/data/conferences/asmep/75837/ on 06/13/2017 Terms of Use: http://www.asme.org/abo